Visualization of Flow Patterns of Cellulose Fiber Suspensions by NMR Imaging

Tie-Qiang Li, Joseph D. Seymour, and Robert L. Powell
Dept. of Chemical Engineering, University of California, Davis, CA 95616

Michael J. McCarthy and Kathryn L. McCarthy
Dept. of Biological and Agricultural Engineering, University of California, Davis, CA 95616

Lars Ödberg
Swedish Pulp and Paper Research Institute, Stockholm, Sweden

Quiescent cellulose fiber suspensions contain regions of relatively high fiber concentration called flocs. Above a critical concentration, which depends on fiber physical properties, such as aspect ratio, shear modulus, and fiber surface chemistry, flocs tend to form a continuous network structure throughout the suspension (Wahren, 1979). During flow, the deformation of the microstructure depends on the relationship between the applied stresses and the interparticle colloidal and mechanical interlocking forces (Norman et al., 1977). Despite extensive study for nearly half a century (Forgacs et al., 1958; Norman et al., 1977), the explicit relationship between the applied stress and the microstructure (rheology) of pulp suspensions remains poorly understood because of the chemical and physical complexity of pulp suspensions and the difficulty in devising experiments in which direct observations of structure and dynamics during flow can be made. Conceptual development has been guided by indirect evidence garnered from studies of steady flow in circular tubes of constant cross section (Forgacs et al., 1958; Norman et al., 1977; Gullichsen and Harkonen, 1981). Depending on the fiber properties, under certain flow conditions all or part of the floc and network structure in the suspension is disrupted, and a completely "fluidized" state is created. However, since pulp suspensions are opaque, it has not been possible to make measurements of velocity profiles. Neither hot film nor laser Doppler anemometry is applicable to cellulose fiber suspensions at concentrations outside the dilute range (Ek et al., 1978). We use NMR imaging to observe the flow of cellulose fiber suspensions undergoing steady, pressure-driven flow in tubes. This technique promises to have a broad impact in a range of studies involving the flow of multiphase systems, such as coal slurries and drilling fluids.

NMR imaging has been widely used for steady laminar flow studies (Caprihan and Fukishima, 1990; Powell et al., 1992), but its application to turbulent flow is rather limited at the present time (Kose, 1991). Using the echo-planar imaging technique, a NMR image can be obtained with an experimental time less than 100 ms, which is of the same order of magnitude as the time scale of turbulent fluctuations. The NMR signals observed in such experiments are therefore "partially averaged," and the signal-to-noise ratio of the reconstructed image is usually too small to be analyzed quantitatively. Although there have been investigations of turbulent flow by NMR spectroscopy without spatial resolution (De Gennes, 1969; Gao and Gore, 1991), joint spatial-velocity NMR images of turbulent flow have not been reported previously. We obtain such images by having the observation time in each phase flow encoding step to be on the order of a few seconds (Li et al., 1993). Here the observation time is defined as the sum of the gradient separation and duration multiplied by the number of the coadded signal acquisitions during the phase flow encoding steps. Extending the observation time allows a statistically averaged stationary signal to be recorded. The reconstructed image from such data gives the mean velocity profile of turbulent flow. Due to the angular symmetry of pipe flow, a joint spatial-velocity 2-D image is sufficient to provide all axial velocity information. This is determined using the spin-echo technique (Hahn, 1950) together with standard frequency position encoding and phase flow encoding (Callaghan, 1991). The essential features of the implemented pulse sequence are given below. A slice of 5 mm was selected in the direction perpendicular to the tube axis using a sin x/x radio frequency pulse and slice selection gradient pulse. Both the slice selection and the frequency encoding gradient pulses were phase-compensated. A sine-shaped bipolar gradient pulse was applied to encode the axial velocity. The two lobes of the phase flow encoding gradient were separated and distributed on each side of a 180° refocusing radio frequency pulse. This optimizes the phase flow encoding time while using a minimum gradient pulse duration. A typical spin echo time and repetition time

Correspondence concerning this work should be addressed to R. L. Powell.

used were 56 and 150 ms, respectively. The flow-phase encoding gradient pulse was incremented 128 times between ±1.0 Gauss/cm in each experiment, and a 256×256 joint spatial-velocity ^{1}H spin density distribution image was obtained after zero-filing and 2-D Fourier transformation.

The time-domain NMR signals observed in an imaging experiment involving steady flow depend primarily on fluid density, $\rho(r)$, and velocity, U, and can be described through (Callaghan, 1991):

$$s(k, p) = \int\int \tilde{\rho}(r)\Gamma(r, U)\exp[-2\pi i(k\cdot r + p\cdot U)]dr dU \quad (1)$$

where

$$\tilde{\rho}(r) = \rho(r)\exp\left\{-t/T_2 - \gamma^2 D_0 \int_0^t \left[\int_0^{t'} G(t'')dt''\right]^2 dt'\right\} \quad (2)$$

$$2\pi k = \gamma \int_0^t G(t')dt' \quad \text{and} \quad 2\pi p = \gamma \int_0^t t' G(t')dt' \quad (3)$$

The product $\tilde{\rho}(r)\Gamma(r, U)$ is the joint spatial-velocity density distribution function; Γ defines the velocity spectrum at a given position r; t is the echo time used in the imaging experiment; and $G(t)$ is the time-dependent magnetic field gradient. The gyromagnetic ratio, the spin-spin relaxation time, and the self-diffusion constant for the ^{1}H in the flow medium are given by γ, T_2, and D_0, respectively. For unsteady or turbulent flow, the instantaneous velocity can be expressed in terms of its average ($\overline{U}$) and an instantaneous deviation (u), and the corresponding NMR signal in an imaging experiment for turbulent flow is given by:

$$s(k, p) = \int\int\int \tilde{\rho}(r)\xi(r, \overline{U})\eta(r, u)\exp \times[-2\pi i(k\cdot r + p\cdot \overline{U} + p\cdot u)]dr d\overline{U} du \quad (4)$$

where ξ and η are the joint probability density distribution functions for $\overline{U}$ and u, respectively. The velocity fluctuations give rise to extra dephasing of the spin magnetization. If the phase-flow encoding time is short, the dephasing varies irregularly. Here, the experimental time is much longer than the time scale of fluctuations and a time-averaged stationary signal is obtained:

$$\overline{s(k, p)} = \int\int \tilde{\rho}(r)\xi(r, \overline{U})\ \overline{\exp(-2\pi i p\cdot u)}\exp \times[-2\pi i(k\cdot r + p\cdot \overline{U})]dr d\overline{U} \quad (5)$$

where the overbar indicates ensemble average. A 2-D Fourier transform of the time-averaged signals gives the mean velocity profile $\xi(r, \overline{U})$ with intensity proportional to $\tilde{\rho}(r)\overline{\exp(-2\pi i p\cdot u)}$. According to Eq. 2, $\tilde{\rho}(r)$ is approximately constant for an incompressible fluid. It can be shown that $\overline{\exp(-2\pi i p\cdot u)}$ depends primarily on the turbulence intensity (root mean square of velocity fluctuations) and the phase-flow encoding gradients (Li et al., 1993).

A 26.2-mm-ID plexiglass pipe was used in a flow loop of 12 m in length. A portion of the tube was in a 2 T Oxford

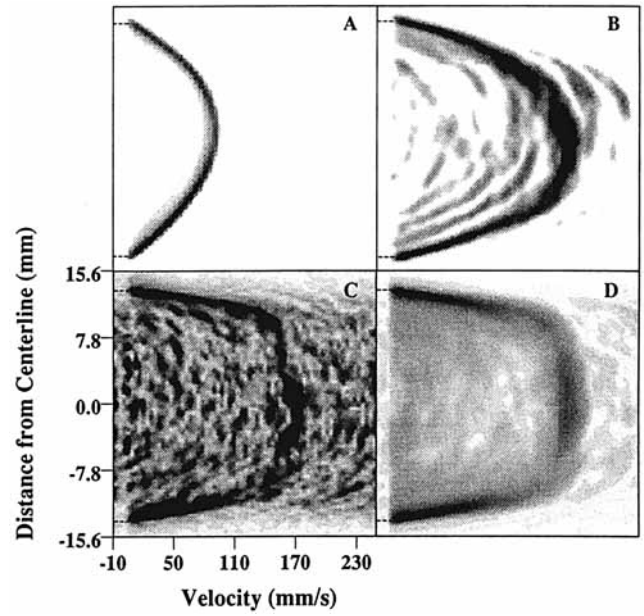

Figure 1. Joint spatial-velocity ^{1}H spin density distribution images of water in inverted-grey scale.

Two signals were accumulated to produce images A, B, and C. 160 signal averages were used for image D. The Reynolds numbers for images A, B, C, and D are 1,250, 2,400, 3,080 and 3,080, respectively. The dash lines indicate the wall boundaries of the tube.

magnet (corresponding to 85.5 MHz ^{1}H resonance frequency), which was connected to a General Electric CSI-II NMR imaging spectrometer. The length of straight pipe preceding the magnet was approximately 4.5 m (L/D = 175), providing sufficient length for the flow profile to be fully developed. A positive displacement variable speed pump (SPS-20, Orange, USA) was used to pump the cellulose fiber suspensions. Suspensions of 0.63% and 0.86% fiber concentration were prepared from bleached hardwood (birch) kraft pulp (Mörrum, Sweden) and bleached softwood (Douglas fir) kraft pulp (Weyerhaeuser, USA), respectively. Distilled water doped with $CuSO_4$ was used to prepare the fiber suspensions. Doping with $CuSO_4$ reduces the relaxation times of the flow medium, which shortens the excitation time of the spin system and allows rapid data acquisition. The receiver/transmitter coil is a home-made 100-mm birdcage coil. Independent estimates of the area-averaged flow rates were carried out by timed collection of the flow material. The volumetric flow rates studied vary from 25.7 to 490.6 mL/s depending on the Reynolds number. The mean flow rates measured by NMR imaging were within the 90% statistical confidence interval of the timed-collection data.

Figure 1 shows flow images of water at different Reynolds numbers, calculated using the bulk flow rates and the tube diameter. At a low Reynolds number (Re = 1,250), a laminar flow profile with evenly distributed intensity was found (Figure 1A). At Reynolds numbers exceeding the critical value (Re ≈2,100) for the onset of turbulence (Brodkey, 1967), blunting and blurring of the velocity profile are found (Figures 1B and 1C). Two signals were coadded to produce images 1B and 1C, and the corresponding observation time in each phase encoding step is 70 ms. Artifacts due to partially averaging the velocity fluctuations, the dark regions not associated with the velocity

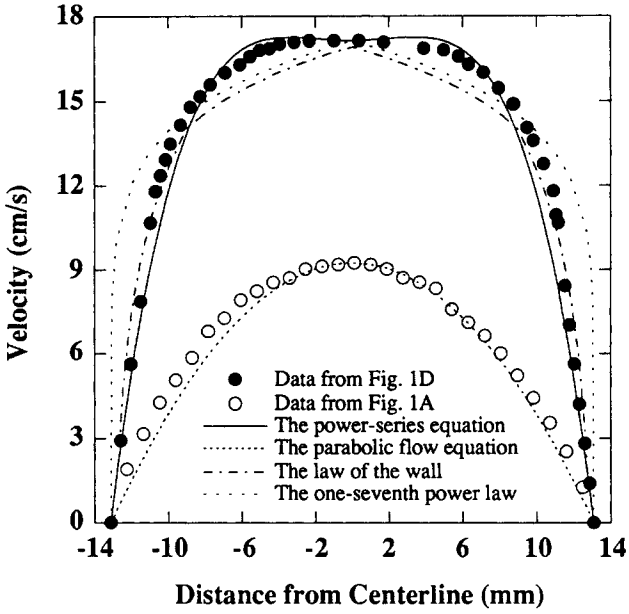

Figure 2. Quantitative analysis of mean velocity distribution obtained from NMR images using different theoretical and empirical models.

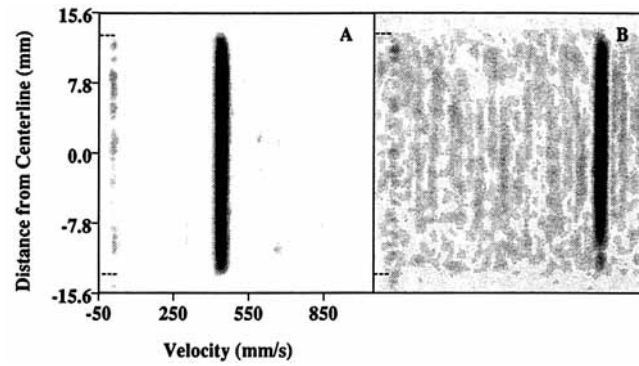

Figure 3. Joint spatial-velocity ^{1}H spin density distribution images of cellulose fiber suspensions prepared from softwood Kraft pulp (Weyerhaeuser, USA) at two different mean flow rates.

The overall fiber concentration of the suspension is 0.86 wt. %. Two signals are averaged to produce images A and B. Image A exhibits a straight vertical line offset to a velocity of 440 mm/s. Image B shows a straight vertical line offset at a velocity of 830 mm/s. Dash lines indicate the wall boundaries of the tube.

profiles, grow rapidly with Reynolds number. At the highest Reynolds numbers, it is no longer possible to clearly discern the profile. To remedy this, the number of coadded signals was increased by a factor of 80, corresponding to an observation time of 5.6 s in each phase encoding increment. The result of this averaging is seen by comparing Figures 1C and 1D. At the same Reynolds number, 3,080, the time-averaged image 1D gives the mean velocity profile, whereas the image obtained from partial averaging is poor. Figure 2 shows that the velocity data from the time-averaged image can be reasonably described by either the one-seventh power law or the law of the wall phenomenological equations (Brodkey, 1967). The best fit, however, is provided by the power series equation (Brodkey, 1967). As discussed above, the intensity of image 1D is unevenly distributed. Intensity losses are the greatest in the outer regions of the viscous sublayer where the turbulence intensity is the highest. The turbulence intensity distribution can be evaluated from the intensity distribution of the time-averaged image by using Eq. 5. The average turbulence intensity for pipe flow has been investigated previously using NMR spectroscopy without spatial resolution (De Gennes, 1969; Gao and Gore, 1991).

The advantage of NMR flow imaging rests with its ability to noninvasively measure velocity profiles in opaque systems. Figure 3 demonstrates this for a softwood pulp suspension with a fiber concentration of 0.86% at two different mean flow rates. For the softwood pulp suspension, there is very little variation in velocity across the tube, with the suspension undergoing intact plug flow (Figures 3A and 3B). The uneven distribution of the shear stress across the tube creates a thin fiber-depleted layer next to the wall where all the shear flow occurs (Norman, et al., 1977). The thickness of this fiber-depleted annulus depends on the strength of the interlocking network formed in the fiber suspension and the applied shear stress (pressure drop or mean velocity). At the mean velocities achieved in the experiments (up to 830 mm/s), this layer is thinner than the pixel size, 196 μm, and cannot be detected by NMR imaging.

Plug flow in fiber suspensions has been inferred from observations of tracer particles near the surface of a transparent tube (Norman, et al., 1977). However, when the mean flow rate is sufficiently high, the fiber network is destroyed, and a complex, unsteady, three-dimensional flow called *mixed flow* is found (Norman et al., 1977; Forgacs et al., 1958). In mixed flow, plug flow in the pipe core is surrounded by an annular region in which water and fibers experience a complex shear flow. Here, it has been hypothesized that turbulence is likely to exist. At still higher velocities, the suspension becomes fully fluidized. The actual flow patterns depend on the fiber properties (such as aspect ratio and flexibility) and concentration. This description of flow patterns in fiber suspensions is somewhat speculative and is based largely on studies of low-consistency suspensions ($<0.5\%$) (Forgacs et al., 1958; Norman et al., 1977) and inferences from indirect measurements of high-consistency suspensions (Bennington et al., 1991).

NMR imaging allows the direct determination of the transition from plug to mixed flow. Figure 4 shows flow images for a 0.63 wt. % hardwood pulp suspension at different mean flow rates. As the mean flow rate is increased, the radius of the plug decreases. At relatively low mean flow rates (Figures 4A and 4B) there is a very thin sublayer adjacent to the pipe wall. An analysis of Figure 4B indicates that the velocity in the sublayer is nearly linear and its thickness is about 0.8 mm (4 pixels) at the mean velocity of 460 mm/s. This is the same order of magnitude as the thickness of the laminar sublayer for pure water at the same average flow rate, as estimated using the law of the wall (Brodkey, 1967). This suggests that the layer next to the pipe wall is fiber-depleted (Norman et al., 1977; Forgacs et al., 1958). Using the sublayer thickness, the mean flow rate, and the viscosity of water, we find that for the flow in Figure 4B, Re = 368, which is very close to the critical value for the onset of turbulence in the sublayer

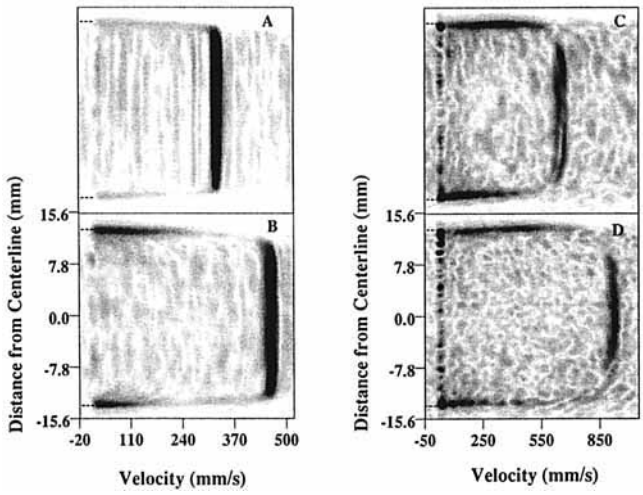

Figure 4. Joint spatial-velocity ^1H spin density distribution images of a cellulose fiber suspension prepared from hardware Kraft pulp (Mörrum, Sweden) at four different mean flow rates.

The overall fiber concentration of the suspension is 0.63 wt. %. Two signals are averaged to produce images A and B. The number of signals averaged to obtain image C and D was increased to 80 and 160, respectively. Dash lines indicate the wall boundaries of the tube.

found in previous studies using fiber suspensions (Norman et al., 1977). The signal losses between the thinned annulus and the plug core are due to velocity fluctuations. Increasing the mean flow rate further decreases the plug diameter and enlarges fiber-depleted regions (Figures 4B-4D).

The number of signals averaged to produce the images in Figures 4C and 4D are 80 and 160, respectively. When such an excessive long-time signal acquisition was used, a band with low signal-to-noise ratio was observed at zero velocity (Figures 4C and 4D). This artifact might be due to the long-term instability of the pump used. At higher mean velocities, only the plug core can be observed with the two scans used to obtain the images shown in Figures 4A and 4B. At the highest average velocity (910 mm/s), the radius of the plug core was reduced to nearly half of the pipe diameter implying that approximately 75% of the suspension was fluidized. Although the signal in the sublayer adjacent to the wall can be enhanced by increasing the number of signals accumulated, it is much more difficult to enhance the signal in the region between the sublayer and the plug core. This may indicate that the particles produce small-scale unsteady motions different from pure water (Seymour et al., 1993).

As shown in Figures 3 and 4, the difference in flows between the softwood and hardwood pulp suspensions is dramatic despite the fact that both suspensions have nearly the same concentration. The typical length of the American Douglas fir fiber is 2-5 mm, which is twice that of the Swedish birch fiber (1-2 mm). Longer fibers mean more contacting points between fibers and hence a stronger fiber network (Wahren, 1979). Classical correlations suggest that such physical differences should account for the observations reported here. We expect that at higher mean flow rates various flow patterns will be observed for the long fiber suspension; however, the accessible mean flow rate is currently limited by the capacity of the pump being used. Finally, by combining NMR imaging measurements with independent pressure drop measurements it will be possible to directly infer rheological parameters, such as the yield stress.

Acknowledgment

Supported by grants from the Swedish Pulp Industry's Foundation for Technical and Forestry Research and Education, NRI Competitive Grants Program/USDA #92-37103-7946 and NSF Award CTS-9057660.

Literature Cited

Bennington, C. P. J., R. J. Kerekes, and J. R. Grace, "Motion of Pulp Fiber Suspension in Rotary Devices," *Can. J. Chem. Eng.*, **69**, 251 (1991).

Brodkey, R. B., *The Phenomena of Fluid Motions*, Addison Wesley, New York (1967).

Callaghan, P. T., *Principles of Nuclear Magnetic Resonance Microscopy*, Clarendon Press, Oxford (1991).

Caprihan, A., and E. Fukushima, "Flow Measurements by NMR," *Phys. Report*, **198**, 195 (1990).

De Gennes, P. G., "Theory of Spin Echoes in a Turbulent Fluid," *Phys. Lett.*, **29A**, 20 (1969).

Ek, R., K. Moller, and B. Norman, "Simultaneous Measurement of Velocity and Concentration in Fiber Suspension Flow," *Proc. Dynamic Flow Conf.*, Marseille, Baltimore (1978).

Forgacs, O. L., A. A. Robertson, and S. G. Mason, "The Hydrodynamic Behavior of Paper-Making Fibres," *Pulp Pap. Mag. Can.*, **59**, 117 (1958).

Gao, J. H., and J. C. Gore, "Turbulent Flow Effects on NMR Imaging: Measurement of Turbulent Intensity," *Med. Phys.*, **18**, 1045 (1991).

Gullichsen, J., and E. Harkonen, "Medium Consistency Technology: I. Fundamental Data," *Tappi J.*, **64**, 69 (1981).

Hahn, E. L., "Spin Echoes," *Phys. Rev.*, **80**, 580 (1950).

Kose, K., "Instantaneous Flow-Distribution Measurements of the Equilibrium Turbulent Region in a Circular Pipe Using Ultra Fast NMR Imaging," *Phys. Rev. A.*, **44**, 2495 (1991).

Li, T. Q., J. D. Seymour, R. L. Powell, K. L. McCarthy, L. Ödberg, and M. J. McCarthy, "Quantification of Turbulent Flow by Phase Encoding NMR Imaging," *SMRM*, **2**, 653 (1993).

Norman, B. G., K. Moller, R. Ek, and G. G. Duffy, "Hydrodynamics of Papermaking Fibres in Water Suspension," *Fiber Water Interactions in Paper-Making*, F. Blolam, ed., Tech. Div., BP&BIF, London (1977).

Seymour, J. D., J. E. Maneval, K. L. McCarthy, M. J. McCarthy, and R. L. Powell, "NMR Velocity Phase Encoded Measurements of Fibrous Suspensions," *Phys. Fluid A*, **5**, 3010 (1993).

Powell, R. L., J. D. Seymour, M. J. McCarthy, and K. L. McCarthy, "Magnetic Resonance Imaging as a Tool for Rheological Measurements," *Proc. of XII Intl. Cong. Rheol.*, Brussels (1992).

Wahren, D., "Fiber Network Structures in Papermaking Operations," The Cutting Edge Conf., Inst. of Paper Chemistry (1979).

Manuscript received July 22, 1993, and revision received Oct. 12, 1993.